HHS Public Access

Author manuscript

Nat Mater. Author manuscript; available in PMC 2018 December 04.

Published in final edited form as:

Nat Mater. 2018 August ; 17(8): 732–739. doi:10.1038/s41563-018-0099-0.

Local immunomodulation with Fas ligand-engineered biomaterials achieves allogeneic islet graft acceptance

Devon M. Headen[1,2,†], **Kyle B. Woodward**[3,†], **María M. Coronel**[1,2,†], **Pradeep Shrestha**[3,†], **Jessica D. Weaver**[1,2], **Hong Zhao**[3], **Min Tan**[3], **Michael D. Hunckler**[1,2], **William S. Bowen**[3], **Christopher T. Johnson**[2,4], **Lonnie Shea**[5], **Esma S. Yolcu**[3], **Andrés J. García**[1,2,*], and **Haval Shirwan**[3,*]

[1]Woodruff School of Mechanical Engineering, Georgia Institute of Technology, Atlanta, GA, USA

[2]Petit Institute for Bioengineering and Bioscience, Georgia Institute of Technology, Atlanta, GA, USA

[3]Institute for Cellular Therapeutics and Department of Microbiology and Immunology, University of Louisville, Louisville, KY, USA

[4]Department of Biomedical Engineering, Georgia Institute of Technology, Atlanta, GA, USA

[5]Department of Biomedical Engineering, University of Michigan, Ann Arbor, MI, USA

Abstract

Islet transplantation is a promising therapy for type 1 diabetes. However, chronic immunosuppression to control rejection of allogeneic islets induces morbidities and impairs islet function. T-effector cells are responsible for islet allograft rejection and express Fas death receptor following activation, becoming sensitive to Fas-mediated apoptosis. Here, we report that localized immunomodulation using microgels presenting an apoptotic form of Fas ligand (SA-FasL) results in prolonged survival of allogeneic islet grafts in diabetic mice. A short course of rapamycin treatment boosted the immunomodulatory efficacy of SA-FasL-microgels, resulting in acceptance and function of allografts over 200 days. Survivors generated normal systemic responses to donor antigens, implying immune privilege of the graft, and had increased $CD4^+CD25^+FoxP3^+$ T-

*Correspondence to: andres.garcia@me.gatech.edu, haval.shirwan@louisville.edu.
†These authors contributed equally.

Author Contributions

D.M.H. and M.M.C. synthesized and characterized SA-FasL-presenting microgels. C.T.J. and M.D.H. performed *in vivo* SA-FasL retention studies. D.M.H., K.B.W., M.M.C., J.D.W., H.Z., P.S., and M.T. performed islet isolation and transplantation studies. W.S.B. produced and qualified SA-FasL protein and K.B.W., P.S. and E.S.Y. performed immuneprofiling analyses. A.J.G., L.S., E.S.Y. and H.S. conceived and designed all experiments. D.M.H., M.M.C., E.S.Y., A.J.G. and H.S. wrote the manuscript.

Competing Financial Interests

H.S. and E.S.Y. hold equity in FasCure Therapeutics, LLC, which has an option to license the SA-FasL technology from the University of Louisville. A patent application titled "FasL-Engineered Biomaterials with Immunomodulatory Function" listing A.J.G., H.S., E.S.Y., D.M.H., and H.Z. has been submitted by the University of Louisville and the Georgia Tech Research Corp based on the results described in this manuscript was submitted on March 9, 2018.

Data Availability Statement

Data supporting the findings of this study are available within the article [and its supplementary information files] and from the corresponding author upon reasonable request.

regulatory cells in the graft and draining lymph nodes. Deletion of T-regulatory cells resulted in acute rejection of established islet allografts. This localized immunomodulatory biomaterial-enabled approach may provide an alternative to chronic immunosuppression for clinical islet transplantation.

Type 1 diabetes (T1D) is an autoimmune disease characterized by loss of insulin-producing β-cell mass, and thereby glycemic control, due to a coordinated immune response against β-cell specific antigens requiring $CD4^+$ T cells [1–3]. Restoration of β-cell mass through allogeneic islet transplantation is currently the preferred clinical intervention to improve glycemic control in patients with severe glycemic instability [4–6]. However, longevity of allogeneic grafts is limited not only by host immune responses, but also by secondary graft failure due to toxic effects of the chronic immunosuppression required to control rejection [7,8]. Pathogenic T effector (Teff) cells are the major culprit of islet allograft destruction [9,10]. Therefore, a promising strategy to increase the functional longevity of islet allografts without the need for long-term immunosuppression comprises therapies that target Teff cells for elimination, mitigating their pathogenic function [11].

Upon activation, T cells upregulate Fas and become sensitive to FasL-mediated apoptosis, a process that plays a critical role in activation-induced cell death (AICD) and tolerance to self-antigens [12]. Deficiency in Fas or FasL results in massive lymphoproliferation and autoimmune pathologies in rodents and humans, demonstrating lack of compensatory mechanisms and the importance of this pathway for immune regulation [13]. Recognizing the immunomodulatory potential of this pathway, several groups have successfully used FasL gene therapy to mitigate allogeneic immune responses for graft acceptance in experimental animal models [14–18]. Although these interventions show efficacy, the unknown safety profile of sustained ectopic expression of FasL in target tissues, as well as technical and regulatory challenges of gene therapy, limit their clinical potential. Additionally, FasL only contributes to AICD in its membrane-bound, oligomeric form [19]. Matrix metalloproteinases (MMP) can cleave FasL into an extracellular soluble form that inhibits apoptosis and acts as a chemoattractant for neutrophils, accelerating the destruction of allografts [20]. To use FasL as an effective immunomodulatory agent, we previously reported the construction of a chimeric form of FasL with streptavidin (SA), SA-FasL, in which the extracellular domain of FasL, lacking MMP sensitive sites, was cloned C-terminal to SA [21]. This protein exists as tetramers and oligomers with robust apoptotic activity on Fas-expressing cells. Pancreatic islets, chemically modified with biotin attached to the cell surface followed by engineering with SA-FasL, acquired an immune privileged status and survived indefinitely under the kidney capsule in the absence of chronic immunosuppression in an allogeneic transplant murine model [22]. This study, however, was limited to islets that were chemically modified to present SA-FasL. Biomaterials engineered to present SA-FasL on their surface as off-the-shelf immunomodulatory products represent a significant advance over chemical modification of islets. This approach eliminates the need for islet chemical modification, which has considerable technical and regulatory challenges, and establishes a translatable and potentially more effective immunomodulatory strategy with improved safety profile for islets. Herein, we engineered a biomaterial for the sustained presentation of SA-FasL within the islet graft microenvironment.

Hydrogel particles for controlled SA-FasL presentation

Hydrogel microparticles (microgels) were synthesized from maleimide-terminated 4-arm poly(ethylene) glycol (PEG-4MAL) macromers using microfluidics polymerization [23]. The PEG-4MAL platform enables stoichiometric, covalent incorporation of thiol-containing molecules and provides improved crosslinking efficiency over other chemistries for formation of structurally defined hydrogels [24]. PEG-4MAL exhibits minimal toxicity *in vivo*, and it is rapidly excreted in the urine [25], important considerations for clinical applications. Biotinylated microgels were produced by reacting biotin-PEG-thiol with PEG-4MAL macromer, and generating 150 μm diameter microgels crosslinked with dithiothreitol (DTT) via microfluidics polymerization (Figure 1a). The resulting microgels displayed covalently-tethered biotin capable of capturing SA with high affinity (Figure 1b). Moreover, biotin-specific capture of SA on microgels varied linearly with concentration of SA in the tethering solution up to a saturating concentration of 150 μg/mL (Figure 1c), demonstrating dose-dependent control of SA presentation on the microgel surface. As expected, capture of SA-FasL on biotinylated microgels obeyed a similar dose-dependent relationship (Supplementary Figure 1). Importantly, display of SA-FasL on microgels induced dose-dependent apoptosis in the A20 murine B-cell lymphoma cells (Figure 1d), which are sensitive to FasL-mediated apoptosis. In contrast to biotin-dependent tethering, direct covalent coupling of SA-FasL to the PEG-4MAL macromer eliminated SA-FasL apoptotic activity (Supplementary Figure 2), demonstrating the importance of biotin immobilization for presentation of bioactive SA-FasL. These results show that SA-FasL tethered to biotinylated microgels retains potent apoptotic activity and that the quantity of bioactive SA-FasL delivered can be easily controlled using this approach.

We cultured rat islets with SA-FasL-presenting microgels (1:2 islet:microgel ratio) for 24 h to examine whether the functionalized material impacts islet health and function. No differences in metabolic activity (Supplementary Figure 3a), glucose-stimulated insulin secretion (Supplementary Figure 3b), secretion of pro-inflammatory cytokines (Supplementary Figure 3c), live-dead staining (Supplementary Figure 3d), or insulin and glucagon expression patterns (Supplementary Figure 3e) were seen between islets co-cultured with SA-FasL-presenting microgels and control free islets. These data demonstrate that SA-FasL-presenting microgels do not negatively impact islet health or function.

We next investigated the retention of SA-FasL presented on microgels *in vivo*. SA-FasL, labelled with a near-infrared fluorescent dye, was immobilized on biotinylated microgels, which were implanted under the kidney capsule of mice. Longitudinal tracking of labelled SA-FasL was performed on an *in vivo* imaging system for 21 days. Images for fluorescent signal show concentrated signal localized to the area around the kidneys in mice receiving labelled SA-FasL-presenting microgels, whereas the fluorescent signal is diffuse for mice receiving labelled free SA-FasL without the microgel carrier (Figure 2a). In mice receiving only labelled SA-FasL, without the microgel delivery vehicle, the protein was rapidly cleared from the transplant site, with a 60% reduction in signal by day 1 post-implantation and negligible signal by day 7 after implantation (Figure 2b). In contrast, mice receiving SA-FasL-presenting microgels displayed significantly higher levels of SA-FasL over time with elevated levels comparable to day 0 signal at the site of implantation over 11 days post-

transplantation. Analysis of retention profiles using single exponential decay curve fits showed significantly longer retention times for SA-FasL-presenting microgels compared to free SA-FasL (half-life 3.0 ± 0.8 days vs. 0.70 ± 0.40 days, $p < 0.0001$). Furthermore, area-under-the-curve calculations demonstrated increased retention of SA-FasL for microgel-tethered vs. free protein (5.25 ± 0.87 vs. 1.98 ± 0.14, $p < 0.007$). We performed histology at sacrifice at day 21 and clearly observe microgels at the implant site (Supplementary Figure 4). This result supports the conclusion that the loss of fluorescence signal for the SA-FasL-microgels arises from unbinding of SA-FasL from the biotinylated microgel and not degradation of the microgels. We expect that this biomaterial strategy for prolonged, local SA-FasL delivery in graft sites significantly enhances the local effects while minimizing risks of systemic effects of this potent immunomodulatory protein.

Immunomodulatory properties of SA-FasL-presenting microgels

The immunomodulatory efficacy of microgels presenting SA-FasL was tested in an allogeneic islet transplantation setting. Unmodified allogeneic BALB/c islets were mixed with microgels, and the resulting mixture was transplanted under the kidney capsule of streptozotocin-diabetic C57BL/6 mice. Mice receiving unmodified islets and control biotinylated microgels acutely rejected all grafts [median survival time (MST) = 15 days; Figure 3a]. Islets co-transplanted with SA-FasL-engineered microgels had significantly prolonged survival (MST = 31 days) with approximately 25% of the subjects surviving over 200 days prior to sacrifice (Figure 3a). Notably, >90% (12/13) of grafts functioned and survived for the entire 200-day observation window in mice co-transplanted with unmodified islets and SA-FasL-presenting microgels when subjects were treated with a short course of rapamycin (0.2 mg/kg daily initiated on day 0 post-transplantation for 15 doses; Figure 3a). Immunostaining of the implant site of recipients with functioning grafts at 200 days revealed insulin-positive structures reminiscent of islets in close association with microgels, whereas no insulin-positive structures were observed in recipients with rejected grafts (Figure 3b). Intraperitoneal glucose tolerance tests demonstrated equivalent function of these long-term grafts compared with naïve mice (Figure 3c); area-under-the-curve analyses showed no differences between naïve and long-term grafts ($P = 0.20$). In marked contrast, the same protocol with rapamycin injections but without SA-FasL-engineered microgels resulted in acute rejection (MST = 36 days) with similar performance as the SA-FasL-presenting microgel group (Figure 3a). Although the mechanistic synergy between SA-FasL and rapamycin in this model is presently unknown and may be complex, death receptor-mediated extrinsic apoptosis in Teff cells by SA-FasL [26] and mitochondria-mediated intrinsic apoptosis by rapamycin [27] are potential candidates. Representative blood glucose levels over time for graft recipients with SA-FasL-presenting microgels + rapamycin or control microgels + rapamycin are shown in Supplementary Figure 5. Nephrectomy in diabetic mice receiving islets and SA-FasL-presenting microgels + rapamycin at day 100 post-transplantation rapidly restored hyperglycemia (Supplementary Figure 6), demonstrating that diabetes reversal in these subjects was due to the graft. Increasing 10-fold the surface density of SA-FasL on microgels had no significant improvement on graft survival (Supplementary Figure 7). We also compared the functional performance of SA-FasL-presenting microgels to SA-FasL-presenting islets as we previously showed that this strategy

was effective in promoting graft acceptance [22]. We observed no differences in the effects of SA-FasL, with or without rapamycin administration, between SA-FasL presented on the surface of islets or microgels (Supplementary Figure 7). However, a major and significant advantage of microgel-based SA-FasL presentation is avoidance of the chemical modification of islets which may overcome a potential negative impact on islet viability and function and also provide a better translatable strategy as an off-the-shelf product. Furthermore, this result shows that SA-FasL does not have to be presented by the target tissue, i.e. islet graft, to overcome immune rejection. Taken together, these results show that simple co-transplantation of allogeneic islets and SA-FasL-engineered microgels restores long-term glycemic control without the use of chronic immunosuppression or islet chemical modification.

Because of the localized nature of immunomodulation, we assessed the systemic response of graft recipients to donor antigens in an *in vitro* proliferation assay (gating strategy for flow cytometric analysis is depicted in Supplementary Figure 8a). Both $CD4^+$ and $CD8^+$ T cells from long-term (> 200 days) islet graft recipients treated with SA-FasL-engineered microgels showed proliferative responses to donor as well as third party antigens (Figure 4a, Supplementary Figure 9). The observed responses were at similar magnitudes to those obtained using T cells from rejecting mice receiving unmodified microgels plus rapamycin. This result indicates that mice receiving SA-FasL-engineered microgels maintain systemic immune competence, and that the protection afforded by SA-FasL-engineered microgels remains localized to the graft, as reported previously in two transplant settings using FasL as an immunomodulatory molecule [22,28].

To further elucidate the mechanism of graft acceptance, immune cell populations harvested from the spleen, graft draining lymph nodes (LNs), and the graft were analyzed using flow cytometry (gating strategy for flow cytometric analysis is depicted in Supplementary Figure 8b), with particular focus on Teff and T-regulatory (Treg) cells as targets of FasL-mediated immunomodulation (Figure 4b, Supplementary Figure 10). We observed a general trend in decreased numbers of both $CD4^+$ and $CD8^+$ Teff cells in tissues of mice receiving SA-FasL-engineered microgels + rapamycin as compared with control group receiving unmodified microgels alone or in combination with rapamycin (Supplementary Figure 11). Interestingly, unmodified microgels plus rapamycin group showed a trend towards increased numbers of Treg cells that reached significance in the graft-infiltrating lymphocytes on day 7 post-transplantation. Treg cells have been shown to be less dependent on mammalian target of rapamycin (mTOR) signaling for proliferation and homeostasis as compared with T conventional cells [29]. Indeed, rapamycin has been used to selectively expand Treg cells both *in vitro* and *in vivo* [30,31]. Under select conditions, rapamycin can positively impact Teff cell memory precursors frequency and long-term survival [32,33]. However, the dose, treatment regimens, and the presence and nature of antigens are important factors impacting the outcome of rapamycin treatment vis-à-vis Treg vs Teff cells [33,34]. Thus, the observed increases in the numbers of both Teff and Treg cells in the control group receiving rapamcyin are not surprising. We observed a trend towards an increased ratio of Treg to $CD4^+$ and $CD8^+$ Teff cells in the graft (Treg:$CD8^+$ Teff) and graft draining LNs (both Treg:Teff populations) in groups receiving SA-FasL-engineered microgels + rapamycin

compared to control groups receiving unmodified microgels alone or in combination with rapamycin (Figure 4b).

Treg cells are required for islet graft acceptance

Treg cells, similar to Teff cells, follow the inflammatory cues and infiltrate into rejecting grafts without a functional consequence [35,36]. Because of the trend in the increased ratio of Treg to Teff cells, we conducted a depletion study to directly assess the role of Treg cells in the observed graft acceptance in our model. For these studies, BALB/c allogeneic islets were transplanted into transgenic C57BL/6 mice expressing human diphtheria toxin (DT) receptor under the control of Foxp3. Unlike antibody-mediated partial Treg cell depletion, this FoxP3/DTR mouse model allows acute ablation of Treg cells and has been used extensively in transplantation and autoimmune settings to assess the role of Treg cells in controlling autoimmunity and graft rejection [37,38]. In these FoxP3/DTR mice, DT administration depletes Treg cells transiently for several days before returning to normal levels (Supplementary Figure 12a). Importantly, DT administration has no effects on the blood glucose levels of FoxP3/DTR mice (Supplementary Figure 12b). Chemically diabetic transgenic mice transplanted with allogeneic islets and SA-FasL-engineered microgels under the transient cover of rapamycin established graft acceptance, as seen previously in C57BL/6 recipients, with mice maintaining graft function at day 50 post-transplantation (Figure 5). Depletion of Treg cells by administration of DT on day 50 resulted in rejection of all grafts by day 82 (Figure 5, MST = 72 days). In marked contrast, control mice without DT treatment maintained graft function for a 200-day experimental end-point. These results provide direct *in vivo* evidence for the dominant role of Treg cells in graft acceptance for mice receiving SA-FasL-presented microgels.

Application to a clinically relevant transplant site

The kidney capsule is an experimentally convenient transplant site to study cell delivery, but it has limitations for clinical adoption. We therefore examined allogeneic islet transplantation into the murine epididymal fat pad. The epididymal fat pad in mice is analogous to the omentum in humans. Importantly, the omentum represents a clinically relevant islet transplant site [39,40]. In order to retain islets in this site, grafts were delivered within a protease-degradable PEG hydrogel with controlled VEGF release that improves islet engraftment [41]. In agreement with our results for the kidney capsule site, allogeneic islets co-transplanted with SA-FasL-microgels under a brief cover of rapamycin treatment showed significantly improved survival in diabetic mice compared to controls ($p < 0.0008$, Figure 6a). The islet grafts in this model also normalized blood glucose levels, demonstrating function (Supplementary Figure 13). It is important to note that the transplant protocol (SA-FasL dose, rapamycin delivery route/regimen) has not been optimized for the epididymal fat pad, and we expect that optimization of these parameters will further improve graft performance in this site. Immunostaining of the transplant site in mice with functioning islets grafts in the SA-FasL-presenting microgels + rapamycin group revealed many structures that stained positive for insulin and glucagon (Figure 6b, isotype controls in Supplementary Figure 14), whereas no such insulin- and glucagon-positive structures were found in mice receiving islets with control microgels. Finally, as an initial assessment of the

potential toxicity of the SA-FasL-microgel treatment, we measured serum levels of liver enzymes and performed histology for liver and kidney in long-term recipients (> 60 days) (Figure 6c). Liver enzyme levels were within the normal range and there were no differences between SA-FasL-presenting microgels and controls. Similarly, there were no differences in gross liver or kidney tissue structure. Taken together, these results demonstrate that the SA-FasL-microgel strategy improves transplanted islet function without chronic immunosuppression in a clinically-relevant transplant site with an acceptable safety profile.

Outlook

The results presented in this study are consistent with the established role of FasL in physiological immune privilege for selected tissues, such as the anterior chamber of the eye and the testes [42–44]. The observed protection against rejection required Treg cells and was localized to the graft, as long-term recipients generated a normal systemic response to the donor antigens, implying immune privilege. This is consistent with a study demonstrating that primary myoblasts transfected to express FasL conferred immune privilege to co-transplanted allogeneic islets [28]. Furthermore, we previously demonstrated that allogeneic islets chemically modified to display SA-FasL protein on their surface under a short cover of rapamycin overcame rejection by inducing graft-localized tolerance and immune privilege, maintained by Treg cells [45].

Engineering microgels with SA-FasL allows controlled loading, presentation, and retention of SA-FasL protein within the graft microenvironment for immunomodulation. This is a unique advantage over gene therapy, because uncontrolled, continuous expression of FasL, which possesses pleiotropic functions and different modes of expression that may be differentially regulated by the target tissues (membrane bound or soluble), may have unintended consequences. Indeed, ectopic expression of FasL using gene therapy for immunomodulation in transplantation settings has resulted in mixed and opposing outcomes with some studies showing a detrimental impact of FasL expression on graft survival [46]. The localized and sustained presentation of SA-FasL with robust apoptotic function using microgels overcomes complications associated with ectopic expression of wild-type FasL in target tissues using gene therapy. This localized immunomodulation concept also limits potential toxicities associated with agonistic antibodies against Fas for immunomodulation [47]. Lastly, SA-FasL-engineered microgels provide the flexibility of an off-the-shelf product for wider clinical applications, as these immunomodulatory materials can be prepared at the time of transplantation and simply co-mixed with islets for delivery without the need of encapsulating islets or chemically modifying islets to present proteins. Importantly, we demonstrate that co-transplantation of SA-FasL-microgels and allogeneic islets in the epididymal fat pad, a clinically relevant transplant site analogous to the omentum in humans, results in graft tolerance and function without chronic immunosuppression. Additional studies in large animal or humanized mouse models will be necessary for further proof-of-efficacy and translation to the clinic.

Methods

Microgel synthesis and characterization

A microgel precursor solution containing 5% w/v PEG-4MAL (20kDa, Laysan Bio) and 1.0 mM biotin-PEG-thiol (1 kDa, Nanocs) was reacted for 15 min in PBS. This precursor was dispersed into droplets and subsequently crosslinked within mineral oil (Sigma) containing 2% SPAN80 (Sigma) and a 1:15 emulsion of 30 mg/mL dithiothreitol (Sigma) on a microfluidic chip, as described previously [23]. Control microgels that did not contain biotin-PEG-thiol were also synthesized. After washing microgels 5 times by centrifugation in 1% bovine serum albumin (Sigma) in PBS, 10^4 microgels were incubated with varying concentrations of a streptavidin-AlexaFluor488 conjugate for 30 min in 500 μL PBS, and were washed 5 times by centrifugation to remove unbound SA. Microgels from each sample were placed in a 96-well plate and fluorescence was measured on a plate reader (Perkin Elmer HTS 7000). Biotin and control microgels were also synthesized with a covalently bound peptide (GRGDSPC)-AlexaFluor594 conjugate for microgel visualization, and were fluorescently imaged to confirm biotin-specific SA immobilization.

In vitro SA-FasL bioactivity

10^4 microgels, with or without biotin, were co-incubated for 30 min in 500 μL PBS with 1% bovine serum albumin containing varying concentrations of SA-FasL. Microgels were washed 8 times by centrifugation to remove unbound SA-FasL, and were incubated with 10^6 A20 cells (ATCC) in 1.0 mL media. After 18 h, cells were stained with markers of early and late apoptosis (annexin V-APC and propidium iodide, BD Biosciences). Samples were analyzed by flow cytometry (Accuri C6 flow cytometer) and cells staining positive for either marker were considered apoptotic. Three independent runs of this experiment were performed with consistent results.

In vitro cytocompatibility of SA-Fas-L conjugated microgels

All animal procedures were performed under protocols approved by the Georgia Institute of Technology IACUC and in accordance with National Institutes of Health guidelines. Rat pancreatic islets were isolated from Lewis male donors (250–300 g, Charles River) and cultured overnight. 500 IEQ in 300 μL of complete CMRL were co-cultured with 1,000 SA-FasL conjugated microgels for an additional 24 h. Islets were then analyzed for metabolic activity via MTT (Promega); Live/Dead samples were visualized using the Viability/Cytotoxicity Kit (Invitrogen) and a Zeiss LSM 710 inverted confocal microscope. A static glucose-stimulated insulin release (GSIR) assay was used to assess the insulin secretion of islets post co-culture, stimulating with low (3 mM) and high Krebs buffer (11 mM) for 1 h each. A second exposure to basal conditions was performed for an additional 1 h. A rat insulin ELISA (Mercodia) was used to quantify GSIR samples. Inflammatory cytokines from co-culture supernatant were analyzed via a multiplexing magnetic bead-based antibody detection kit (Milliplex Rat Cytokine Panel with IFNg, IL-1b, IL-6, IL-17A, MCP-1, MIP-1a) following the manufacturer's instructions. Fifty microliters of supernatant from three independent wells were analyzed using a Magpix with Analyst analysis software (Milliplex@ 5.1, Merck). Standard curves for each analyte were generated using standards provided by manufacturer. Immunostaining analysis of insulin and glucagon was performed

post co-culture by fixing islet samples in 10% formalin for 1 h. Whole samples were stained in suspension for insulin (Dako A0564, 1:100), glucagon (Abcam ab10988, 1:50) and DAPI (Invitrogen, 1:500). Whole mount samples were imaged for insulin (yellow), glucagon (magenta) and DAPI (blue). *In vitro* cytocompatibility data was collected from 2 independent islet isolation experiments, with representative data presented as the mean ±SD of group replicates (n = 3 biological independent samples for each group).

In vivo SA-FasL tracking

SA-FasL was labelled with AlexaFluor750 NHS Ester (Thermo Fisher), and free dye was removed by desalting in Zeba column (7k MWCO, Thermo Fisher) three times. 3.0 μg of labelled SA-FasL was immobilized onto 2,000 biotin microgels by incubation for 30 min followed by 5 wash steps. Microgels presenting SA-FasL or free SA-FasL were implanted under the kidney capsule of C57Bl/6 recipients (n=8 mice/group), and signal intensity and distribution were monitored longitudinally using an IVIS SpectrumCT imaging system (Perkin-Elmer). Intensity measurements were normalized to day 0 values. Non-linear single exponential decay curve fits were performed in GraphPad Prism and retention time was compared using a t-test. Area-under-the-curve metric was calculated for each group, and a Welch's t-test was used to compare groups.

Islet transplantation

All animal procedures were performed under protocols approved by the University of Louisville and Georgia Institute of Technology IACUC and in accordance with National Institutes of Health guidelines. BALB/c pancreatic islets were isolated using Liberase TL as a digestive enzyme (Roche Life Science) and purified by a Ficoll density gradient as previously published [21]. To biotinylate islets, overnight cultured islets were incubated in 5 μM EZ-Link Sulfo-NHS-LC- Biotin (Thermo Scientific) for 30 min at room temperature, washed extensively with PBS to remove unbound biotin solution. Biotinylated islets and microgels were engineered with SA-FasL (~150 ng/500 islets and 1–10 μg/1,000 microgels). For kidney capsule experiments, 500 islets were co-transplanted with 1,000 microgels into streptozotocin diabetic (200 mg/kg i.p., diabetes [> 250 mg/dL] confirmed on two consecutive days) C57BL/6 or B6.129(Cg)- $Foxp3^{tm3(DTR/GFP)Ayr}$/J (C57BL/6.$FoxP3^{EGFP/DTR}$) recipients, where indicated. For Treg depletion, islet graft recipients were injected i.p. with diphtheria toxin (50 μg/kg body weight) and depletion was confirmed in peripheral blood lymphocytes using flow cytometry. Selected groups were also treated i.p. with rapamycin at 0.2 mg/kg daily for 15 doses starting the day of transplantation. Unmodified BALB/c islets co-transplanted with unmodified microgels were used as controls. For epididymal fat pad transplantation, a 2-cm incision was made in the lower abdomen and the epididymal fat pads were exposed. Microgels (1,200 microgels conjugated with SA-FasL) and 600 IEQ were placed in each fat pad, which was then sealed with an *in situ* crosslinked PEG hydrogel containing VEGF [41]. The incision was sutured, and the skin closed using surgical staples. Blood glucose and body weight of recipients were monitored in every morning. Blood glucose levels ≥ 250 mg/dL for two consecutive daily measurements were considered rejected. IPGTT was performed on day 200 post-transplantation after 6 h fasting using 2 g/kg glucose solution (25%). Blood glucose levels were assessed by tail prick before injection and 10, 20, 30, 60, 90, 120 min after injection.

Data was graphed using GraphPad Prism and the Mantel-Cox test was used to determine significance between groups, $p < 0.05$ was considered significant. For some epididymal fat pad transplants (2 mice/group), blood samples were collected at 50–70 days post-transplantation. Anesthesia was induced by administering xylazine/ketamine, after which animals were bled via a cardiac puncture. Blinded blood samples were deposited in serum separator tubes and sent to ANTECH Diagnostics for analysis. Full necropsies were also performed for evidence of any gross abnormalities post-transplantation. Explanted kidneys and livers were preserved in 10% formalin solution and processed and stained with hematoxylin and eosin. Microscopy was performed using an optical microscope (Zeiss 510), and the images were taken using Axio Vision software. Images presented are representative of all samples collected (n=8 mice/group).

Immune monitoring

Spleen, kidney, and kidney draining lymph nodes were harvested from rejecting and long-term mice (> 200 days). Single cells were prepared from the spleen and lymph nodes by gentle mechanical dispersion and from islet-harboring kidneys by collagenase digestion. Cells were stained using antibodies to cell surface markers (Alexa 700-CD4 Ab 1:200 BD Bioscience 557956, APC-Cy7-CD8 Ab 1:100 BD Bioscience 557654, PE-Cy7-CD25 Ab 1:100 from Pharmingen 25-0251-82, BD, and eFlour 450-CD44 Ab 1:100 eBiosicences 48-0441-82 and PerCP-Cy5.5- CD62L Ab at 1:200 from eBioscience 45-0621-82). Intracellular FoxP3 staining was carried out on fixed/permeablized cells using FoxP3 Transcription Factor Staining Buffer set (diluted 1:20, eBioscience 11-5773-82). Data was collected using BD LSR II and analyzed using Diva software and FlowJo 9.8. Data was graphed using GraphPad Prism and t tests with Welch's correction were used to determine significance between groups, $p < 0.05$ was considered significant.

Proliferation assay

Splenocytes harvested from selected group of transplant recipients from different isolations were labeled with carboxyfluorescein succinimidyl ester (CFSE) and used as responders to irradiated (2000 cGy) splenocytes from donor or third party C3H mice in a standard *in vitro* proliferation assay [21]. Groups tested were microgel plus rapa (n=3), SA-FasL-microgel (n=5), SA-FasL-microgel plus rapa (n=5). After 4 days in culture, cells were stained with 7AAD and fluorescence-conjugated antibodies against CD4 (1:200 BD Bioscience 557956) and CD8 (1:100, BD Biosicence 557654), and analyzed for CFSE dilution by gating on live cells using BD LSR II. Data was analyzed using Diva software. Data was graphed using GraphPad Prism and Welch's t test was used to determine significance between groups, $p < 0.05$ was considered significant.

Confocal Microscopy

After the observation period of 200 days, long-term islet bearing kidneys were snap frozen in OCT compound (Sakura Tissue-Tek) by submerging in methyl butane (Sigma) on dry ice. Tissues were cut in 10 μm-thick slices using a Bright OTF5000 cryomicrotome (Rose Scientific) and put on frosted slides for staining. Slides were fixed in 4% paraformaldehyde, incubated in 0.5% Triton X-100, and blocked in 0.1% bovine serum albumin, 5% goat serum, and rat anti-mouse CD16/CD32 (BD Pharmingen). Staining was performed using

rabbit anti-glucagon monoclonal antibody (Cell Signaling 8233S, 1:100) and guinea pig anti-insulin polyclonal antibody (Dako A0564, 1:100) as primary antibodies, followed by washing and staining with AlexaFluor-647-conjuaged goat anti-rabbit antibody (Life Technologies A21244, 1:100) and AlexaFluor-555-conjugated anti-guinea pig antibody (Invitrogen A21435, 1:300). Hoechst 33342 (Molecular Probes H3570, 1:25) was used to stain DNA. Fluorescent images were obtained using a Leica TCS SP5 confocal microscopy under 10X magnification.

Statistical Analyses

Statistical analyses were applied to biologically independent samples (separate wells of samples, plates of cells, or mice) from every single experiment. Experiments were repeated at least twice, and the numbers of repeats are indicated in figure legends. For all *ex vivo* islet studies, at least 3 biological replicates were used across 2 different islet isolations. For *in vivo* data, groups comprise transplants across multiple islet isolations and sample size was determined based on power calculations to detect 20% differences among means using variances from previous/pilot experiments. Animals were randomized among control and treatment groups keeping the initial average weight and blood glucose levels at similar level for all groups. All animals were used for analysis unless the mice died or had to be euthanized because of pre-defined euthanasia criteria (significant weight loss, unresponsive to external stimuli) according to IACUC-approved protocols. Treated diabetic animals that did not achieve primary function (defined as 5 consecutive blood glucose readings <250 mg/dL) were excluded from analysis as this is an effect related to poor isolation outcomes and tissue quality and not the experimental groups being evaluated. Blood glucose measurements were performed by blinded and non-blinded personnel in a random fashion. Animals were checked in a rotation schedule by 4 different users. All blood glucose measurements were electronically and time-stamped recorded. Sample size for each experimental group and the statistical test used to determine significant differences among groups are reported in the appropriate figure legend. GraphPad Prism 7 was used for data analysis and representation, and $p < 0.05$ was considered statistically significant. Non-parametric tests were used if the data did not meet the assumptions of ANOVA, and two-tailed pair-wise comparisons using Bonferroni or Tukey's tests were used. For t tests, Welch's correction was used if the SD for the two groups were not equivalent.

Supplementary Material

Refer to Web version on PubMed Central for supplementary material.

Acknowledgments

This work was funded in part by the Juvenile Diabetes Research Foundation (2-SRA-2014-287-Q-R) and NIH (R21EB020107, R21AI113348, R56AI121281, and U01AI132817). Funding from the NIH Innovation and Leadership in Engineering Technologies and Therapies Postdoctoral Training (T90 DK097787 to M.M.C.), a JDRF Postdoctoral Fellowship (J.D.W.), the NIH Ruth L. Kirschstein National Research Service Award (F30AR069472 to C.T.J.), and a National Science Foundation Graduate Fellowship (M.D.H.) is greatly appreciated. We thank the core facilities at the Parker H. Petit Institute for Bioengineering and Bioscience at the Georgia Institute of Technology for the use and assistance with their shared equipment, services, and expertise.

References

1. Nakayama M, Beilke JN, Jasinski JM, Kobayashi M, Miao D, Li M, et al. Priming and effector dependence on insulin B : 9-23 peptide in NOD islet autoimmunity. J Clin Invest. 2007; 117(7): 1835–1843. [PubMed: 17607359]
2. Roep BO, Arden SD, Devries RRP, Hutton JC. T-cell clones from a type-1 diabetes patient respond to insulin secretory granule proteins. Nature. 1990; 345(6276):632–634. [PubMed: 2190098]
3. Yoon JW, Yoon CS, Lim HW, Huang QQ, Kang Y, Pyun KH, et al. Control of autoimmune diabetes in NOD mice by CAD expression or suppression in beta cells. Science. 1999; 284(5417):1183–1187. [PubMed: 10325232]
4. Alejandro R, Lehmann R, Ricordi C, Kenyon NS, Angelico MC, Burke G, et al. Long-term function (6 years) of islet allografts in type 1 diabetes. Diabetes. 1997; 46(12):1983–1989. [PubMed: 9392484]
5. Boggi U, Vistoli F, Amorese G, Giannarelli R, Coppelli A, Mariotti R, et al. Long-term (5 years) efficacy and safety of pancreas transplantation alone in type 1 diabetic patients. Transplantation. 2012; 93(8):842–846. [PubMed: 22314339]
6. Shapiro AMJ, Ricordi C, Hering BJ, Auchincloss H, Lindblad R, Robertson P, et al. International trial of the edmonton protocol for islet transplantation. N Engl J Med. 2006; 355(13):1318–1330. [PubMed: 17005949]
7. Radu RG, Fujimoto S, Mukai E, Takehiro M, Shimono D, Nabe K, et al. Tacrolimus suppresses glucose-induced insulin release from pancreatic islets by reducing glucokinase activity. Am J Physiol-Endocrinol Metab. 2005; 288(2):E365–E371. [PubMed: 15479952]
8. Hernandez-Fisac I, Pizarro-Delgado J, Calle C, Marques M, Sanchez A, Barrientos A, et al. Tacrolimus-induced diabetes in rats courses with suppressed insulin gene expression in pancreatic islets. Am J Transplant. 2007; 7(11):2455–2462. [PubMed: 17725683]
9. Haskins K, McDuffie M. Acceleration of diabetes in young NOD mice with a CD4+ islet-specific T-cell clone. Science. 1990; 249(4975):1433–1436. [PubMed: 2205920]
10. Roep BO, Stobbe I, Duinkerken G, van Rood JJ, Lernmark A, Keymeulen B, et al. Auto- and alloimmune reactivity to human islet allografts transplanted into type 1 diabetic patients. Diabetes. 1999; 48(3):484–490. [PubMed: 10078547]
11. Yolcu ES, Ash S, Kaminitz A, Sagiv Y, Askenasy N, Yarkoni S. Apoptosis as a mechanism of T-regulatory cell homeostasis and suppression. Immunol Cell Biol. 2008; 86(8):650–658. [PubMed: 18794907]
12. Ju ST, Panka DJ, Cui HL, Ettinger R, Elkhatib M, Sherr DH, et al. Fas(CD95) FasL interactions required for programmed cell-death after T-cell activation. Nature. 1995; 373(6513):444–448. [PubMed: 7530337]
13. Brunner T, Mogil RJ, Laface D, Yoo NJ, Mahboubi A, Echeverri F, et al. Cell-autonomous Fas (CD95) Fas-ligand interaction mediates activation-induced apoptosis in T-cell hybridomas. Nature. 1995; 373(6513):441–444. [PubMed: 7530336]
14. Arai H, Chan SY, Bishop DK, Nabel GJ. Inhibition of the alloantibody response by CD95 ligand. Nat Med. 1997; 3(8):843–848. [PubMed: 9256273]
15. Lau HT, Yu M, Fontana A, Stoeckert CJ. Prevention of islet allograft rejection with engineered myoblasts expressing FasL in mice. Science. 1996; 273(5271):109–112. [PubMed: 8658177]
16. Matsue H, Matsue K, Walters M, Okumura K, Yagita H, Takashima A. Induction of antigen-specific immunosuppression by CD95L cDNA-transfected 'killer' dendritic cells. Nat Med. 1999; 5(8):930–937. [PubMed: 10426318]
17. Min WP, Gorczynski R, Huang XY, Kushida M, Kim P, Obataki M, et al. Dendritic cells genetically engineered to express Fas ligand induce donor-specific hyporesponsiveness and prolong allograft survival. J Immunol. 2000; 164(1):161–167. [PubMed: 10605007]
18. Tourneur U, Malassagne B, Batteux F, Fabre M, Mistou S, Lallemand E, et al. Transgenic expression of CD95 ligand on thyroid follicular cells confers immune privilege upon thyroid allografts. J Immunol. 2001; 167(3):1338–1346. [PubMed: 11466351]

19. O'Reilly LA, Tai L, Lee L, Kruse EA, Grabow S, Fairlie WD, et al. Membrane-bound Fas ligand only is essential for Fas-induced apoptosis. Nature. 2009; 461(7264):659–663. [PubMed: 19794494]
20. Ottonello L, Tortolina G, Amelotti M, Dallegri F. Soluble Fas ligand is chemotactic for human neutrophilic polymorphonuclear leukocytes. J Immunol. 1999; 162(6):3601–3606. [PubMed: 10092820]
21. Yolcu ES, Askenasy N, Singh NP, Cherradi SE, Shirwan H. Cell membrane modification for rapid display of proteins as a novel means of immunomodulation: FasL-decorated cells prevent islet graft rejection. Immunity. 2002; 17(6):795–808. [PubMed: 12479825]
22. Yolcu ES, Zhao H, Bandura-Morgan L, Lacelle C, Woodward KB, Askenasy N, et al. Pancreatic islets engineered with SA-FasL protein establish robust localized tolerance by inducing regulatory T cells in mice. J Immunol. 2011; 187(11):5901–5909. [PubMed: 22068235]
23. Headen DM, Aubry G, Lu H, García AJ. Microfluidic-Based Generation of Size-Controlled, Biofunctionalized Synthetic Polymer Microgels for Cell Encapsulation. Adv Mater. 2014; 26(19): 3003–3008. [PubMed: 24615922]
24. Phelps EA, Enemchukwu NO, Fiore VF, Sy JC, Murthy N, Sulchek TA, et al. Maleimide cross-linked bioactive PEG hydrogel exhibits improved reaction kinetics and cross-linking for cell encapsulation and in situ delivery. Adv Mater. 2012; 24(1):64–70. 62. [PubMed: 22174081]
25. Phelps EA, Headen DM, Taylor WR, Thule PM, Garcia AJ. Vasculogenic bio-synthetic hydrogel for enhancement of pancreatic islet engraftment and function in type 1 diabetes. Biomaterials. 2013; 34(19):4602–4611. [PubMed: 23541111]
26. Ju ST, Panka DJ, Cui H, Ettinger R, el-Khatib M, Sherr DH, et al. Fas(CD95)/FasL interactions required for programmed cell death after T-cell activation. Nature. 1995; 373(6513):444–448. [PubMed: 7530337]
27. Yellen P, Saqcena M, Salloum D, Feng J, Preda A, Xu L, et al. High-dose rapamycin induces apoptosis in human cancer cells by dissociating mTOR complex 1 and suppressing phosphorylation of 4E-BP1. Cell Cycle. 2011; 10(22):3948–3956. [PubMed: 22071574]
28. Lau HT, Yu M, Fontana A, Stoeckert CJ Jr. Prevention of islet allograft rejection with engineered myoblasts expressing FasL in mice. Science. 1996; 273:109–112. [PubMed: 8658177]
29. Zeiser R, Leveson-Gower DB, Zambricki EA, Kambham N, Beilhack A, Loh J, et al. Differential impact of mammalian target of rapamycin inhibition on CD4+CD25+Foxp3+ regulatory T cells compared with conventional CD4+ T cells. Blood. 2008; 111(1):453–462. [PubMed: 17967941]
30. Battaglia M, Stabilini A, Roncarolo MG. Rapamycin selectively expands CD4+CD25+FoxP3+ regulatory T cells. Blood. 2005; 105(12):4743–4748. [PubMed: 15746082]
31. Basu S, Golovina T, Mikheeva T, June CH, Riley JL. Cutting edge: Foxp3-mediated induction of pim 2 allows human T regulatory cells to preferentially expand in rapamycin. J Immunol. 2008; 180(9):5794–5798. [PubMed: 18424697]
32. Rao RR, Li Q, Odunsi K, Shrikant PA. The mTOR kinase determines effector versus memory CD8+ T cell fate by regulating the expression of transcription factors T-bet and Eomesodermin. Immunity. 2010; 32(1):67–78. [PubMed: 20060330]
33. Araki K, Turner AP, Shaffer VO, Gangappa S, Keller SA, Bachmann MF, et al. mTOR regulates memory CD8 T-cell differentiation. Nature. 2009; 460(7251):108–112. [PubMed: 19543266]
34. Hurez V, Dao V, Liu A, Pandeswara S, Gelfond J, Sun L, et al. Chronic mTOR inhibition in mice with rapamycin alters T, B, myeloid, and innate lymphoid cells and gut flora and prolongs life of immune-deficient mice. Aging Cell. 2015; 14(6):945–956. [PubMed: 26315673]
35. Bunnag S, Allanach K, Jhangri GS, Sis B, Einecke G, Mengel M, et al. FOXP3 expression in human kidney transplant biopsies is associated with rejection and time post transplant but not with favorable outcomes. Am J Tranplant. 2008; 8(7):1423–1433.
36. Yapici U, Bemelman FJ, Scheepstra CG, Roelofs JJ, Claessen N, van der Loos C, et al. Intragraft FOXP3 protein or mRNA during acute renal allograft rejection correlates with inflammation, fibrosis, and poor renal outcome. Transplantation. 2009; 87(9):1377–1380. [PubMed: 19424039]
37. Kim JM, Rasmussen JP, Rudensky AY. Regulatory T cells prevent catastrophic autoimmunity throughout the lifespan of mice. Nat Immunol. 2007; 8(2):191–197. [PubMed: 17136045]

38. Lahl K, Loddenkemper C, Drouin C, Freyer J, Arnason J, Eberl G, et al. Selective depletion of Foxp3+ regulatory T cells induces a scurfy-like disease. J Exp Med. 2007; 204(1):57–63. [PubMed: 17200412]

39. Baidal DA, Ricordi C, Berman DM, Alvarez A, Padilla N, Ciancio G, et al. Bioengineering of an Intraabdominal Endocrine Pancreas. N Engl J Med. 2017; 376(19):1887–1889. [PubMed: 28489987]

40. Berman DM, Molano RD, Fotino C, Ulissi U, Gimeno J, Mendez AJ, et al. Bioengineering the Endocrine Pancreas: Intraomental Islet Transplantation Within a Biologic Resorbable Scaffold. Diabetes. 2016; 65(5):1350–1361. [PubMed: 26916086]

41. Weaver JD, Headen DM, Aquart J, Johnson CT, Shea LD, Shirwan H, et al. Vasculogenic hydrogel enhances islet survival, engraftment, and function in leading extrahepatic sites. Sci Adv. 2017; 3(6):e1700184. [PubMed: 28630926]

42. Stuart PM, Griffith TS, Usui N, Pepose J, Yu X, Ferguson TA. CD95 ligand (FasL)-induced apoptosis is necessary for corneal allograft survival. J Clin Invest. 1997; 99(3):396–402. [PubMed: 9022072]

43. Griffith TS, Brunner T, Fletcher SM, Green DR, Ferguson TA. Fas ligand-induced apoptosis as a mechanism of immune privilege. Science. 1995; 270(5239):1189–1192. [PubMed: 7502042]

44. Takeda Y, Gotoh M, Dono K, Nishihara M, Grochowiecki T, Kimura F, et al. Protection of islet allografts transplanted together with Fas ligand expressing testicular allografts. Diabetologia. 1998; 41(3):315–321. [PubMed: 9541172]

45. Yolcu ES, Zhao H, Bandura-Morgan L, Lacelle C, Woodward KB, Askenasy N, et al. Pancreatic Islets Engineered with SA-FasL Protein Establish Robust Localized Tolerance by Inducing Regulatory T Cells in Mice. J Immunol. 2011; 187(11):5901–5909. [PubMed: 22068235]

46. Kang SM, Schneider DB, Lin Z, Hanahan D, Dichek DA, Stock PG, et al. Fas ligand expression in islets of Langerhans does not confer immune privilege and instead targets them for rapid destruction. Nat Med. 1997; 3(7):738–743. [PubMed: 9212099]

47. Ogasawara J, Watanabe-Fukunaga R, Adachi M, Matsuzawa A, Kasugai T, Kitamura Y, et al. Lethal effect of the anti-Fas antibody in mice. Nature. 1993; 364(6440):806–809. [PubMed: 7689176]

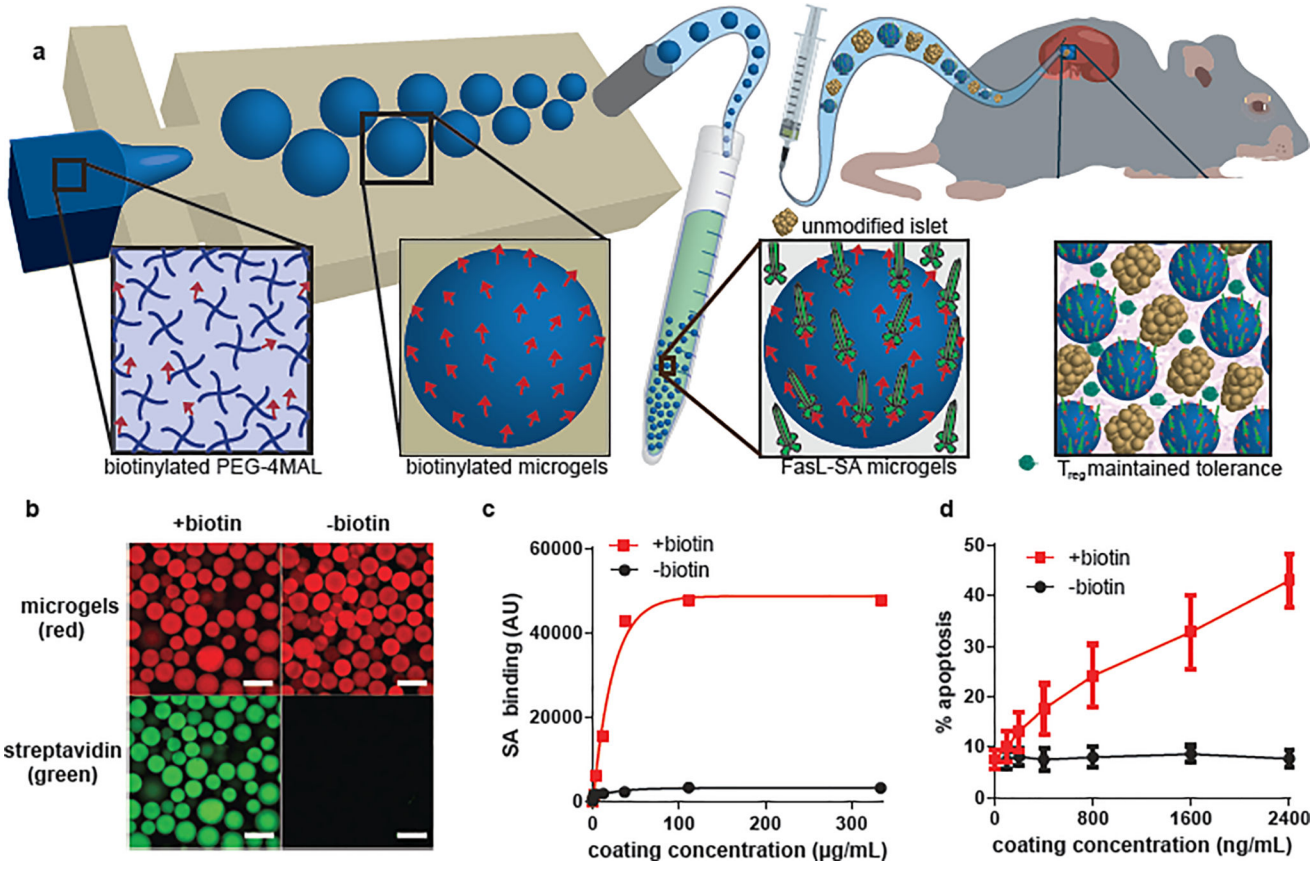

Figure 1. Microgels for controlled presentation of immunomodulatory proteins

(**a**) Flow focusing microfluidics were used to generate biotinylated microgels from biotin-functionalized PEG-4MAL macromers. SA-FasL was immobilized on microgels and these immunomodulatory microgels were co-transplanted with islets under the kidney capsule of diabetic mice inducing graft acceptance. (**b,c**) Biotinylated microgels capture and display SA in a dose-dependent manner until reaching saturation (scale bar 200 μm). Representative experiment (n=3 samples, mean ± SD) shown from 3 independent runs with consistent results. (**d**) SA-FasL presented on microgels maintains bioactivity and induces dose-dependent apoptosis in FasL-sensitive cells. Representative experiment (n=3 samples, mean ± SD) shown from 3 independent runs with consistent results.

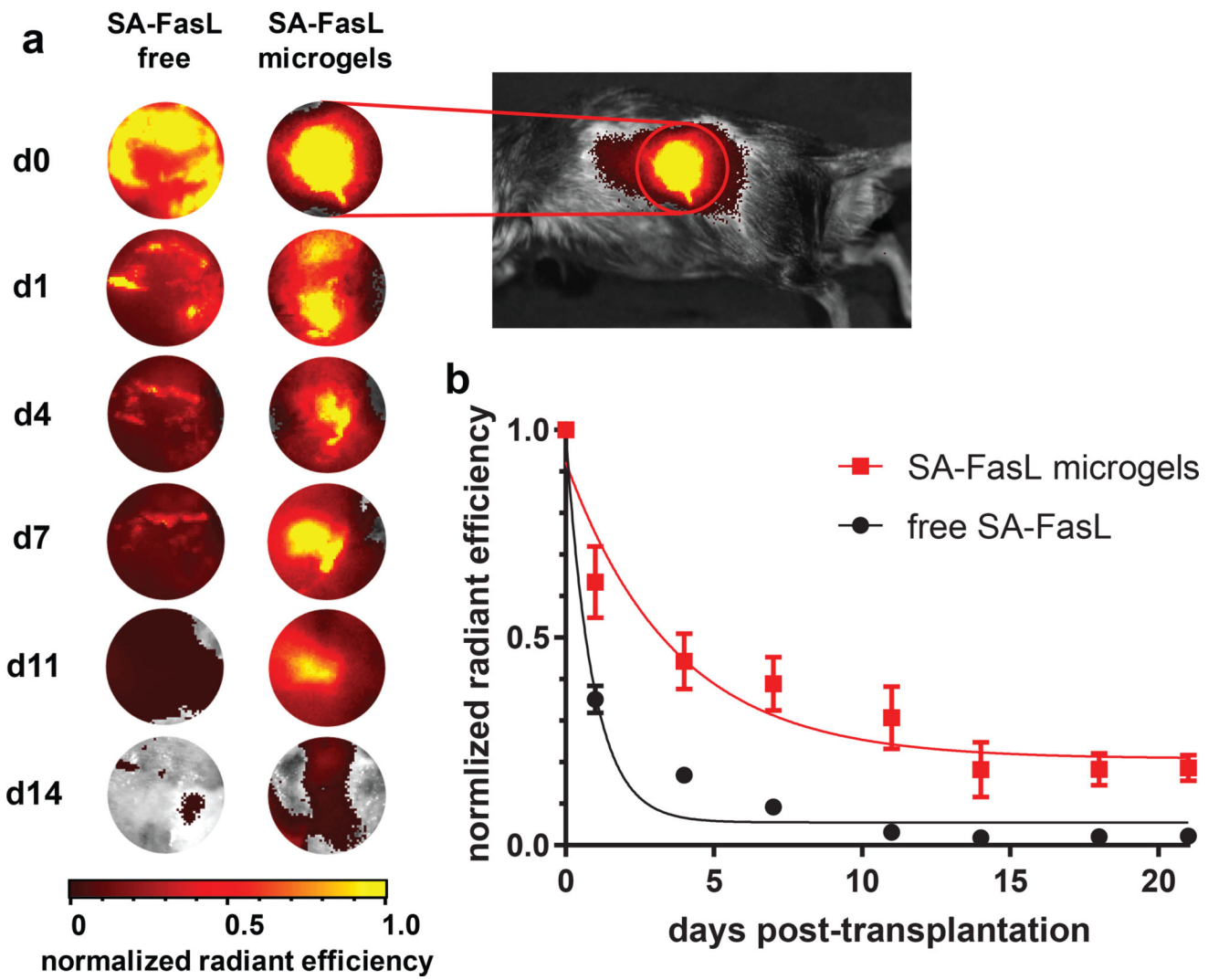

Figure 2. Microgels prolong SA-FasL retention *in vivo*

SA-FasL was labelled with a near-IR dye and implanted under the kidney capsule of mice and imaged *in vivo*. (**a**) Representative images show localization of SA-FasL to graft site when presented on microgels, in contrast to diffuse signal measured in animals receiving free SA-FasL. Heat maps are consistent across animals in the same treatment group. Images are not shown for days 18 and 21 because signal was negligible. (**b**) Quantification of *in vivo* fluorescence and exponential decay curve fit demonstrate that microgels presenting SA-FasL prolong protein retention compared to free SA-FasL. Representative experiment (n=8 mice/group, mean ± SE; F-test (DFn, DFd) = 20.39 (2, 124) for curve fit parameters, two-tailed $p < 0.0001$) shown from 2 independent runs with consistent results.

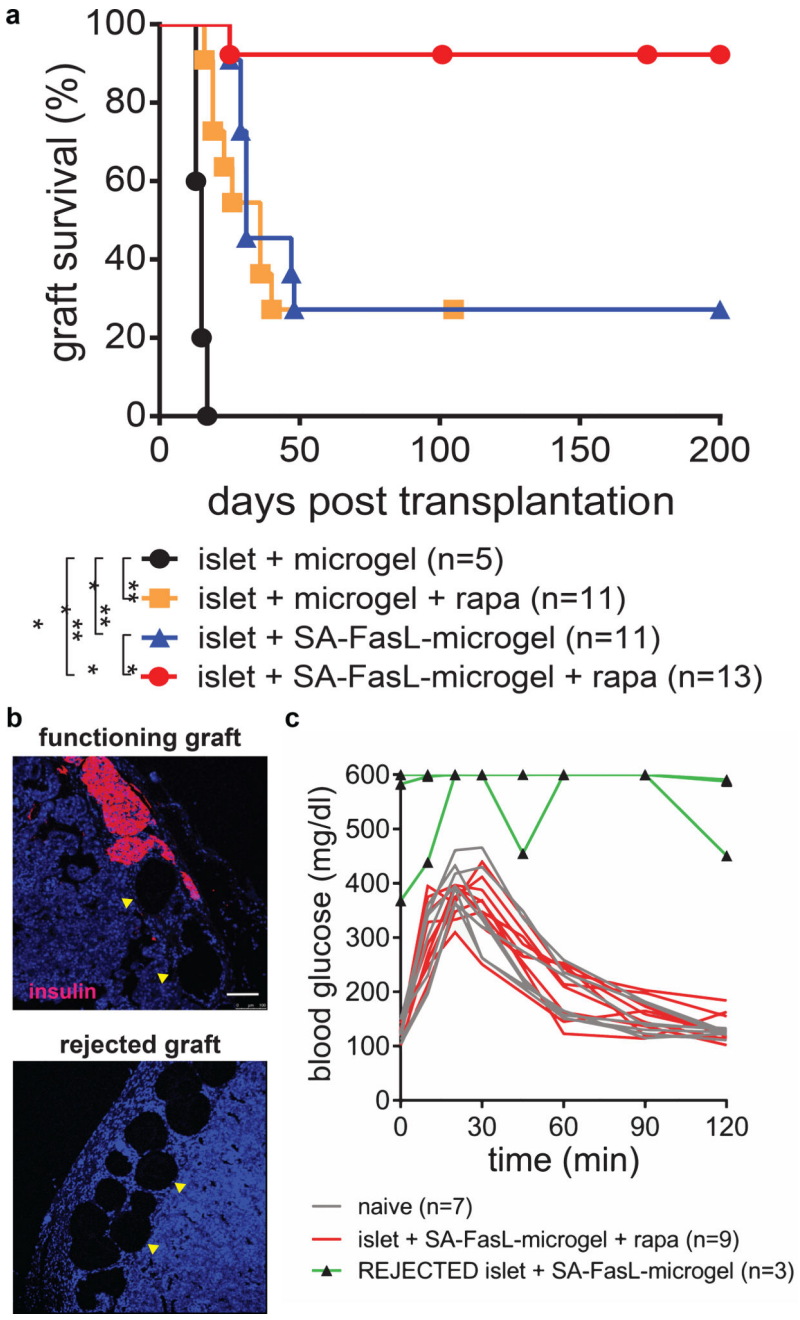

Figure 3. Survival of allogeneic islet grafts co-transplanted with SA-FasL-presenting microgels

(**a**) Islet graft survival. SA-FasL-presenting or control microgels and unmodified BALB/c islets were co-transplanted under the kidney capsule of chemically diabetic C57BL/6 recipients. Rapamycin was used at 0.2 mg/kg daily i.p. injection for 15 doses starting the day of transplantation in the indicated groups. Animals were monitored for blood glucose levels and two consecutive daily readings of ≥ 250 mg/dL were considered to be diabetic (rejection). Data comprise transplants performed from various islet isolations with sample size indicating number of treated mice. Survival curves were analyzed using Mantel-Cox test ($\chi^2 = 59.98$, df = 3, $p < 0.0001$; two-tailed pair-wise comparisons with Bonferroni's

correction, $p < 0.0001$, $^{**}p < 0.01$, $^{***}p < 0.001$). (**b**) Immunostaining of a long-term functioning graft (> 200 days) and rejected graft from recipients receiving SA-FasL-presenting microgels showing insulin (red) positive structures and DNA (blue) (scale bar 100 μm). Yellow arrowheads indicate microgels. Staining patterns are consistent for samples across different independent runs. (**c**) Intraperitoneal glucose tolerance test on day 200 showing long-term islet grafts with function equivalent to naïve subjects (sample size indicates number of mice evaluated, area-under-the-curve metric was computed using trapezoid rule in GraphPad Prism and compared using the z-statistic, two-tailed $p = 0.20$).

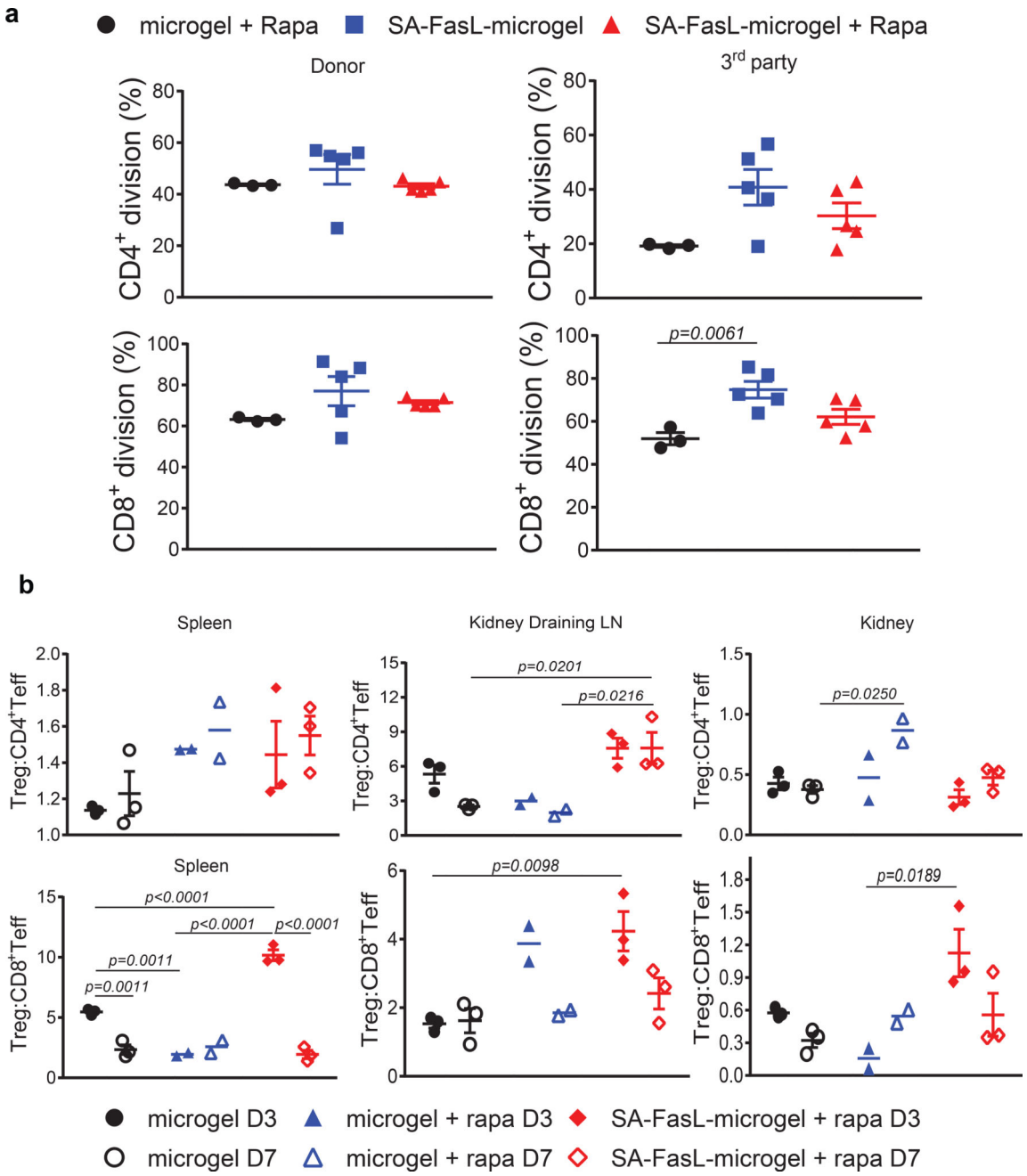

Figure 4. Immune monitoring and the role of CD4$^+$CD25$^+$FoxP3$^+$ Treg cells in islet graft acceptance

(**a**) Systemic response of long-term graft survivors to donor antigens. Carboxyfluorescein succinimidyl ester (CFSE)-labeled splenocytes were used as responders to irradiated BALB/c donor and C3H third party stimulators in an *ex vivo* mixed lymphocyte reaction assay. The dilution of CFSE dye in CD4$^+$ and CD8$^+$ T cells was assessed using antibodies to CD4 and CD8 molecules in flow cytometry and plotted as percent division for each cell population (n=3 mice/group for microgel and n=5 mice/group for microgel + rapa and SA-FasL-microgel + rapa; mean ± SE; ANOVA with two-tailed pair-wise comparisons using Tukey's test). (**b**) Analysis of Teff and Treg cells. Single cells prepared from the spleen,

kidney, and kidney-draining lymph nodes of the indicated groups on day 3 and 7 post-islet transplantation were stained with fluorescence-labelled antibodies to cell surface molecules that define $CD4^+$ Teff ($CD4^+CD44^{hi}CD62L^{lo}$), $CD8^+$ Teff ($CD8^+CD44^{hi}CD62L^{lo}$), and Treg ($CD4^+CD25^+FoxP3^+$) populations and analyzed using flow cytometry. The ratios of Treg to $CD4^+$ Teff and $CD8^+$ Teff are plotted (n=2 mice/group for microgel + rapa and n=3 mice/group for microgel and SA-FasL-microgel + rapa; mean ± SE; ANOVA with two-tailed pair-wise comparisons with Bonferroni's correction).

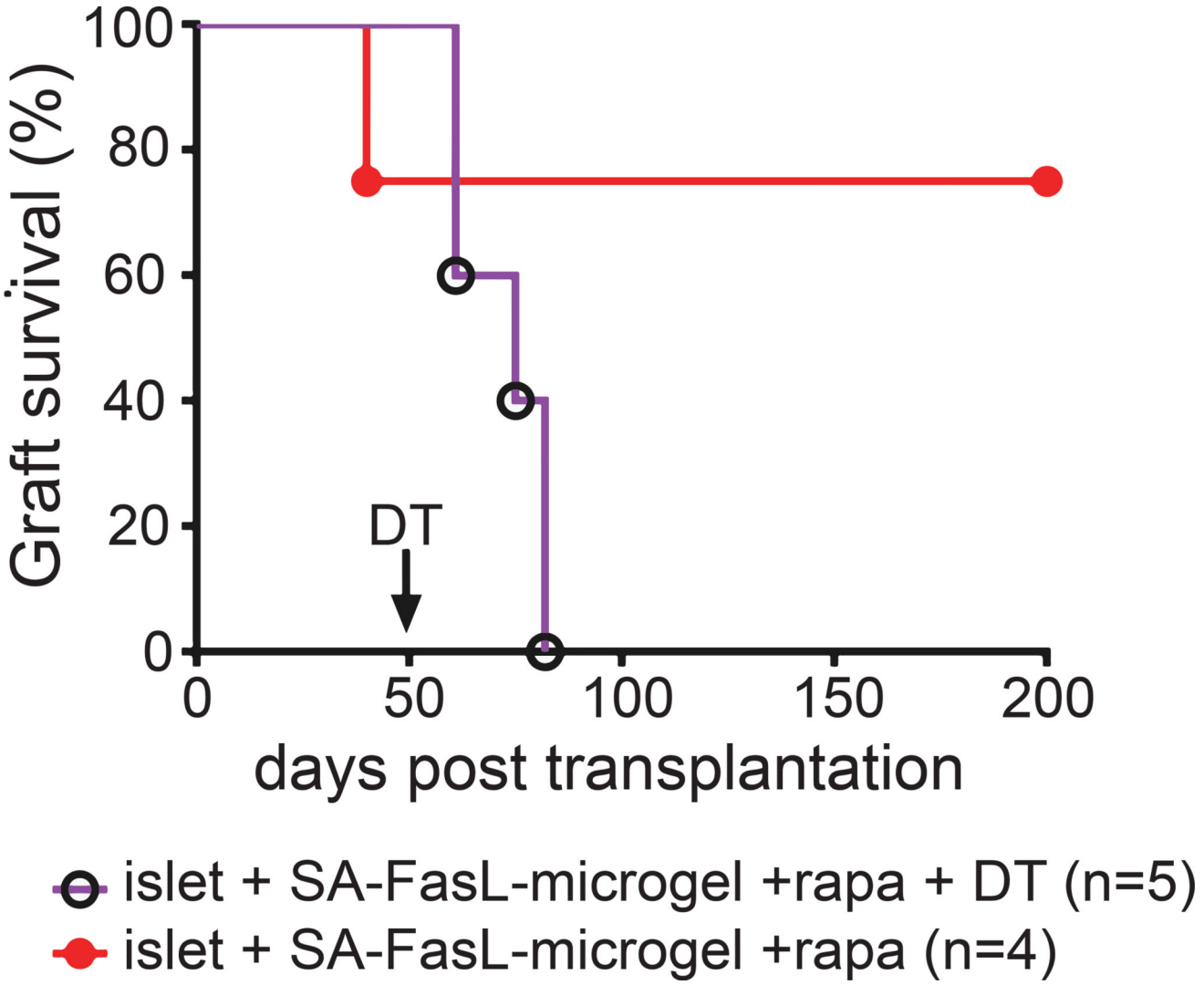

Figure 5. Treg cells are required for islet graft acceptance

Depletion of Treg cells results in acute rejection of established islet grafts. C57BL/6.FoxP3$^{EGFP/DTR}$ mice were transplanted with BALB/c islets and SA-FasL-presenting microgels under transient cover of rapamycin (administered i.p. daily at 0.2 mg/kg for 15 doses). A cohort of mice (n=5) was injected i.p. with 50 μg/kg diphtheria toxin on day 50 post-transplantation (arrow) to deplete Treg cells, while another group (n=4) was left untreated. Data comprise transplants performed from various islet isolations with sample size indicating number of treated mice. Survival curves post day 50 were analyzed using Mantel-Cox test ($\chi^2 = 6.26$, df = 1, $p < 0.0123$).

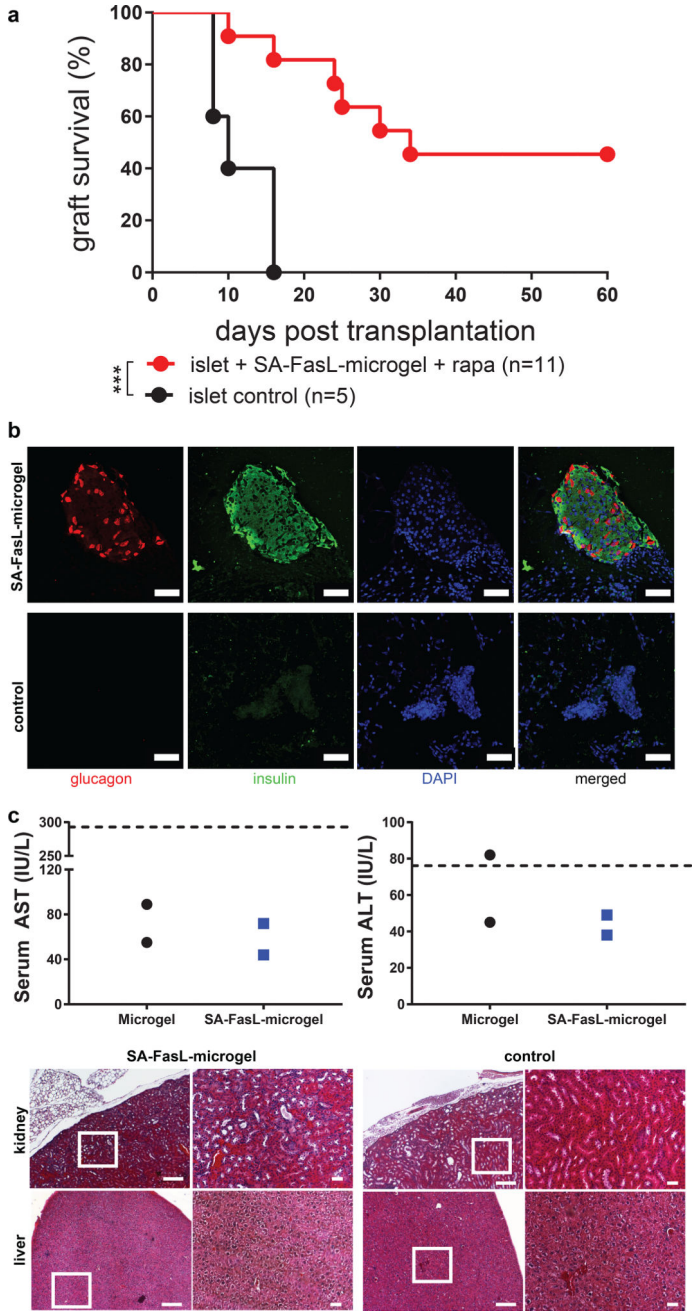

Figure 6. Immune acceptance of allogeneic islet grafts co-transplanted with SA-FasL-presenting microgels in the epididymal fat pad

(**a**) Islet graft survival. SA-FasL-engineered microgels and unmodified BALB/c islets were co-transplanted in the epididymal fat pad of chemically diabetic C57BL/6 recipients. Rapamycin was used at 0.2 mg/kg daily i.p. injection for 15 doses starting the day of transplantation. Animals were monitored for blood glucose levels and two consecutive daily readings of ≥ 250 mg/dL were considered to be diabetic (rejection). Data comprise transplants performed from various islet isolations with sample size indicating number of treated mice. Survival curves were analyzed using Mantel-Cox test ($\chi^2 = 11.28$, df = 1, $p < 0.0008$). (**b**) Immunostaining of a long-term functioning graft (> 60 days) from mice

receiving SA-FasL-presenting microgels + rapamycin showing glucagon (red) and insulin (green) positive structures and DNA (blue) (scale bar 50 μm). Staining patterns consistent for samples across different independent runs. (**c**) Serum liver enzyme levels showing no differences between SA-FasL-presenting microgel and control groups (n=2 mice/group from 2 separate islet transplantations). Hashed line denotes normal upper enzyme levels. Histological sections (left: low magnification, scale bar 200 μm; right: higher magnification of boxed area, scale bar 50 μm) for kidney and liver. Histological staining patterns are consistent for samples across 2 separate islet transplantations.